arXiv:1301.7074v1 [gr-qc] 29 Jan 2013

Gravitational and electromagnetic outputs from binary neutron star mergers

Carlos Palenzuela[1], Luis Lehner[2], Marcelo Ponce[3], Steven L. Liebling[4],
Matthew Anderson[5], David Neilsen[6], and Patrick Motl[7]
[1]Canadian Institute for Theoretical Astrophysics, Toronto, Ontario M5S 3H8, Canada,
[2]Perimeter Institute for Theoretical Physics,Waterloo, Ontario N2L 2Y5, Canada
[3]Department of Physics, University of Guelph, Guelph, Ontario N1G 2W1, Canada,
[4]Department of Physics, Long Island University, New York 11548, USA
[5] Pervasive Technology Institute, Indiana University, Bloomington, IN 47405, USA
[6]Department of Physics and Astronomy, Brigham Young University, Provo, Utah 84602, USA,
[7]Department of Science, Mathematics and Informatics, Indiana University Kokomo, Kokomo, IN 46904, USA,

The late stage of an inspiraling neutron star binary gives rise to a strong emission of gravitational waves due to its highly dynamic, strong gravity. Interactions between the stellar magnetospheres, driven by the extreme dynamics, can produce considerable outflows. We study the gravitational and electromagnetic waves produced during the inspiral and merger of a binary neutron star system using a full general relativistic, resistive MHD evolution code. We show that the interaction between the stellar magnetospheres extracts kinetic energy from the system and powers radiative Poynting flux and heat dissipation. These features depend strongly on the configuration of the initial stellar magnetic moments. Our results indicate that this power can strongly outshine pulsars in binaries and has a distinctive angular and time-dependent pattern.

PACS numbers:

Introduction: Binary systems involving neutron stars are among the most likely sources of detectable gravitational waves, making them important sources for gravitational wave detectors such as Advanced LIGO. Gravitational wave observations of neutron star binaries are expected in the next few years, and the combination of these data with electromagnetic observations will provide new opportunities to study the fundamental physics of these stars, and their interactions with their environments. As an example of the important interplay between gravitational wave (GW) and electromagnetic (EM) data, consider models of compact object mergers for short, hard gamma ray bursts (SGRBs) (see e.g. [1] for a review). If the initial binary consists of two neutron stars, the merger may result in either the immediate collapse to a black hole or the creation of an intermediate, hyper-massive neutron star, supported by thermal pressure and differential rotation, followed by a delayed collapse to a black hole. The interaction of the central compact object with a magnetic field can power radiation with the hard spectrum and short time scales characteristic of SGRBs. Considerable effort has been devoted to understanding these bursts, concentrating on emission after the merger. Recently however, there has also been a significant interest in possible EM emissions preceding the merger. This has been motivated, in part, by both the desire to maximize opportunities for gravitational and electromagnetic waves detection, as well as surveys for EM transients that may be precursors to SGRBs (e.g [2]) and other transients from compact binary mergers (e.g. [3]). A basic question here is what possible mechanisms prior to merger can yield sufficiently strong EM emissions to be detected. These detection might be aided by GW observations, which in future years will provide timing information, sky localization, and other physical parameters to aid in identifying sources (e.g. [3–6]).

Precursor emissions may be generated by crust cracking due to resonance effects [7] or magnetosphere interactions [8–12]. A particularly appealing mechanism, *unipolar induction*, relies on the extraction of a star's kinetic energy by the magnetically dominated magnetosphere surrounding the stars. Here an "effective circuit" is established between the stars, powered by an electromotive force produced by the relative motion of a weakly, or non-magnetized star through the magnetic field of the other, allowing for energy dissipation. The energy released by this circuit either reaches its maximum prior to merger or gives rise to episodic emissions depending on the resistance of the circuit. Different models build upon this possibility [10–12], predicting a transient preceding the merger on a time of a few seconds, possibly accompanied by a radio signal.

The expected luminosity for a binary system composed by a magnetized primary star and an unmagnetized secondary one is roughly given by [12],

$$L_{\rm ind} \sim 7\times 10^{40}\,\xi\,(B^*_{11})^2\,\left(a_{30\,{\rm km}}\right)^{-13/2}\ {\rm ergs/s}, \qquad (1)$$

where ξ gives the azimuthal twist of flux tubes connecting both stars, B^* the magnetic field strength of the primary star and we have assumed typical sizes $R_* = R_c = 10$ km and masses $M_* = M_c = 1.4\,M_\odot$ for the stars. A key unknown here is the azimuthal twist which depends on the total resistance of the circuit. For a free-space magnetosphere $\xi = 64\pi v_{\rm rel}$, where $v_{\rm rel}$ the relative velocity between the stars, and the resultant luminosity is

$L_{\rm ind} \sim 1.7 \times 10^{40}\,(B^{*}_{11})^2 a^{-7}_{30\,{\rm km}}$ ergs/s. The above estimate assumes a quasi-adiabatic process, with an unmagnetized companion so that the induced circuit can be analyzed in simple terms. However a richer structure should arise when both stars are magnetized; in particular, significant reconnections of the magnetic field lines can take place, which would depend on the orientation of magnetic moments. Estimates of these are difficult to obtain, requiring numerical solutions to unravel the possible phenomenology.

To study EM emission from dynamic neutron star systems, it is crucial to properly model global electromagnetic fields, as well as gravitational and hydrodynamic effects. That is, to consistently incorporate magnetic fields present in the stars, their effects in the magnetosphere region surrounding the compact objects (see discussion in [13]), the rapidly changing, and extreme, gravitational fields involved, as well as the magnetized matter describing the stars. We have done so using general relativity coupled to relativistic, resistive magnetohydrodynamics in full 3D. Details of our implementation and work building up to it can be found in [13–20].

Approach and techniques: We study inspiraling, magnetized binary neutron stars, concentrating on the pre-merger epoch, and monitor closely the EM and GW radiation produced by the system, the ensuing current sheets, dissipation layers, and reconnection regions. We focus on a binary initially described by a pair of equal mass neutron stars in a quasicircular orbit, with an initial separation $L = 45$ km, corresponding to an orbital frequency $\Omega_o = 1.85$ rad/ms. The geometric and matter initial data for this system are obtained with the LORENE library [21], assuming a polytropic equation of state $P = K\rho^{\Gamma}$ with $\Gamma = 2$ and $K = 123$. The individual stars have a baryonic mass $M = 1.62\,M_{\odot}$, radius $R_{*} = 13.6$ km, and a magnetic moment μ_i that produces a dipolar magnetic fields B^i in each star's comoving frame. The magnetic moment is related to the radial magnetic field at the pole of the star B_{*} by the relation $\mu = B_{*} R_{*}^3$. In our simulations we set $B_{*} = 1.5 \times 10^{11}$ G, a values on the high end of observations from binaries but still realistic. The electric field is obtained from the ideal MHD condition $\mathbf{E} = -\mathbf{v} \times \mathbf{B}$, where the velocity in the star is given by the orbital motion, and we assume the magnetosphere is initially at rest. Our numerical domain extends up to $L = 320$ km and contains five nested fixed mesh refinement (FMR) grids, each finer grid with twice the resolution of its parent grid, such that the highest resolution grid has $\Delta x = 0.45$ km and extends up to 58 km, covering both stars and the inner part of the magnetosphere. We compute the Poynting-vector luminosity at three different surfaces, the furthest located at $R_{\rm ext} = 180$ km.

We consider three related initial configurations of the magnetic moments to gain insight into the overall behavior of magnetized binaries: aligned and equal magnetic moments (Case U/U) with $\mu_1 = \mu_2 = \mu$, anti-aligned and equal magnetic moments (Case U/D) with $\mu_1 = -\mu_2 = \mu$, and aligned magnetic moments with one-dominant moment (Case U/u) with $\mu_1 = 100\,\mu_2 = \mu$. The direction of the magnetic moments is given with respect to the orbital angular momentum direction.

Results: In all cases, the magnetic field strengths have a negligible effect on the orbital dynamics of the system up to merger [14, 22], as their contribution to the total inertia is several orders of magnitude below the matter contribution. Consequently, the three cases we study progress to merger in exactly the same way, producing the same gravitational signal. The stars orbit each other, and as a consequence of gravitational waves carry both binding energy and angular momentum, the system merges in ≈ 2.5 orbits. At this point we stop our simulations (leaving the post-merger epoch for future work).

While the orbiting behavior is the same for all three cases considered, the electromagnetic field dynamics and magnetosphere interactions depend sensitively on the orientation of the magnetic dipolar moment of the stars. Such interactions affect strongly the resulting field's topology and induced dissipation regions, reconnections of field lines, and net Poynting flux, as well as other relevant features. At a basic level, the accelerated orbital motion of the stars induces only a small degree of winding along its magnetic field lines; thus the magnetospheres essentially co-rotate with the stars and the magnetic field at their surfaces (and therefore, the magnetic dipolar moments) remains almost constant until the merger.

In the anti-aligned case (U/D), a shear layer is induced at the midplane, separating two regions filled with magnetically dominated plasma moving in opposite directions. The poloidal component of the magnetic fields points in opposite directions in the midplane, allowing for reconnections that consequently connect both stars (see Fig. 1). Further, the binary's rotation stretches these magnetic field lines -increasing their tension- and gives rise to a toroidal magnetic field that, beyond some distance from the orbital center and in the plane connecting both stars, has equal signs above the equator and the opposite sign below. The region near the stars, and especially near the orbital plane, is more complicated. Reconnections at the midplane seed a current sheet that propagates outwards forming a spiral pattern. Interestingly, the current sheet structure rotates with the periodicity of the orbital motion, effectively providing a "spacetime tracer", that would induce distinct features in possible EM signals from these systems.

When the magnetic moments are aligned and equal (Case U/U), a shear layer is also induced in the midplane between the stars due to the relative opposite velocities of the magnetospheres. (See Fig. 1.) However, in this case the symmetry and consequent magnetic repulsion between aligned field lines prevents reconnections between the stars. Again, rotation induces a toroidal magnetic field, although the topology is clearly different than the one observed in the U/D case. Here the structure is reminiscent of the aligned (dipole) rotator [23]. This is natural, as there is a net effective dipole at leading order with $\mu_{\rm eff} = 2\mu$. However in this case the symmetry of the system implies an (approximate) periodicity in the solution given by half the orbital period. A current sheet is also induced at the equatorial plane. This current sheet arises at far distances first (defining the light cylinder), and closes in as the orbit tightens, displaying a behavior analogous to the current sheet of an aligned rotator. Again the binary's dynamics modifies the structure and behavior of this current sheet. A spiral pattern results from the inhomogeneous structure of the electromagnetic fields produced by the binary structure and the orbital motion.

When the first star has a dominant magnetic field moment and the second star is significantly less magnetized (Case U/u), the magnetic field of the first star eventually dominates that of the companion even near its surface. A net magnetic flux from the stronger magnetized star threads the weakly magnetized star, and a circuit can be established. As a consequence, global electromagnetic field features are roughly given by the inspiraling dipole together with the induction on the other star. An interesting effect arises as magnetic fields from the strongly magnetized star slide off the companion's surface and reconnect afterwards. This produces a dissipation tail as illustrated in Fig. 1. This tail gradually grows in extent as the merger progresses, populating a current sheet.

The qualitative understanding of the radiation from these three systems, including the angular distribution, can be obtained from the Poynting flux shown in Fig. 2. Both the U/D and U/U cases radiate more strongly along the shear layer between the two stars, while the U/u case does so mainly on the equatorial plane and primarily in the direction of the strongly magnetized star. The radiation in the U/D and U/U cases is partially collimated. The flux density in a polar cap (with opening angle of $\Theta_o < 30^o$) is larger than the average by 2.5 and 1.9, accounting for 1/3 and 1/4 of the total power, respectively. The radiation from the U/u case is emitted mainly near the equatorial plane, with 2/3 of the total energy radiated between $60^o < \Theta_o < 90^o$.

The total Poynting luminosity (Fig. 3) in time shows several important features. First, the U/D case is significantly more radiative than the U/U case. This is interesting as the "inner-engine" in both cases is powered by the fields of each star and the orbital motion, which are the same in both cases (modulo the field topologies), implying a more efficient tapping of orbital energy with anti-aligned magnetic moments (Case U/D) when they are aligned (Case U/U), possibly due to the energy stored as toroidal magnetic tension in the U/D case.

To explain the observed phenomenology, guidance can be drawn by considering an effective magnetic moment and how it radiates within a force-free magnetosphere. In particular, recall that an aligned (dipolar) rotator within force-free radiates a power $L_{\rm dip} \approx \mu^2\Omega^4$ [23]. Since the U/U case has, to leading order, a rather constant effective magnetic dipole $\mu_{\rm eff} = 2\mu$, one can expect $L^{U/U}_{\rm dip} \approx \Omega^4$. This behavior is consistent with our results for such case at late times, as can be observed in Fig. 3. The anti-aligned configuration U/D is more in-

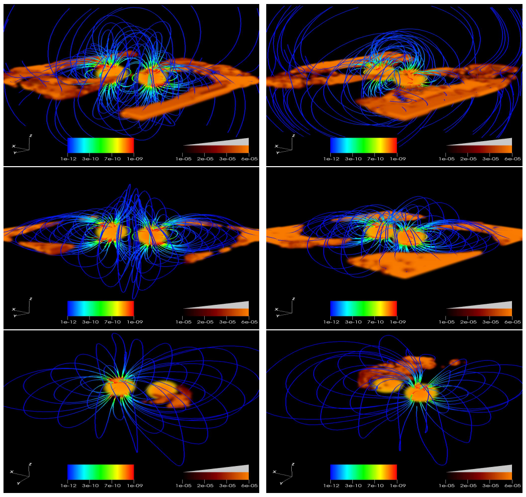

FIG. 1: Magnetic field configurations (field lines) and current sheets (orange regions) for the U/D (top panel), U/U (mid panel) and U/u (bottom panel) respectively at times t=3.6ms and t=4.7 ms. A shear layer is induced in a midplane between the stars in the U/D and U/U cases, with reconnections given rise to field lines connecting both stars in the U/D (top panel) and repulsion between the magnetic fields in the U/U case (middle panel). A dissipation tail emanates behind the weakly magnetized star (bottom panel).

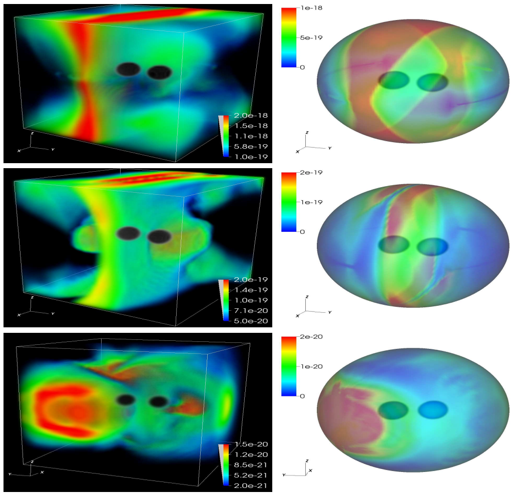

FIG. 2: Poynting flux for the *U/D* (top panel), *U/U* (mid panel) and *U/u* (bottom panel) case at $t = 4.1$ ms, in a volume (left panels) and evaluated in a sphere located at $r = 80$ km (right panels).

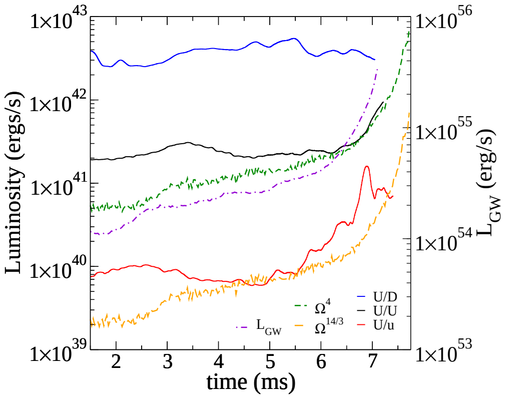

FIG. 3: The gravitational (right axis) and electromagnetic (left axis) luminosities for the three different magnetic field configurations, together with two curves with Ω^4 and $\Omega^{14/3}$ dependency.

volved, since the leading order of the effective dipolar moment vanishes and higher order terms need to be considered. For a rotating quadrupole, $L_{\rm quad} \approx Q^2\Omega^6$, with Q a measure of the magnetic quadrupole from the system, which scales as d^4 (with d the characteristic size of the quadrupolar source). An effective quadrupole could be defined here as the stars approach each other and fields reconnect. The characteristic size of the effective quadrupole necessarily scales with the binary's separation (a), though the magnetic field, as sourced by the individual stars, remains fairly constant. Thus, one would expect $L_{\rm quad} \approx a^8\Omega^6 \simeq \Omega^{2/3}$ (using the Keplerian relation $a \propto \Omega^{-2/3}$). This results in a rather flat profile within the frequencies spanned by the system in its last 2.5 orbits, consistent with the observed behavior.

However, in the U/u case this picture is not quite applicable. Here the dominant field is given by a non-rotating star and, as opposed to the other cases, the contribution of both stars does not give rise to an effective rotation to define a light cylinder before merger. Nevertheless, the unipolar induction model can be adopted. This model, using again the Keplerian relation, leads to an estimated luminosity $L^{\rm U/u}_{\rm ind} \approx \Omega^{14/3}$. This behavior fits reasonably well the observed late time behavior, as shown in Fig. 3.

Notably, a circuit seems to be established in all cases (see Fig. 4), albeit with different characteristics. In both the U/U and U/D cases, the circuit is established in between the stars and along the axial directions, while in the U/u case the circuit closes between the stars. Additionally, in the U/u case the amount of energy dissipated as Joule Heating ($J_i E^i$) is comparable to the Poynting energy radiated. For the U/D and U/U cases, on the other hand, the energy dissipated as heat is only a fraction of the radiated energy, between 25–50%. This indicates that magnetosphere interactions in the U/D and U/U cases induce more radiation than can be explained via an unipolar induction model.

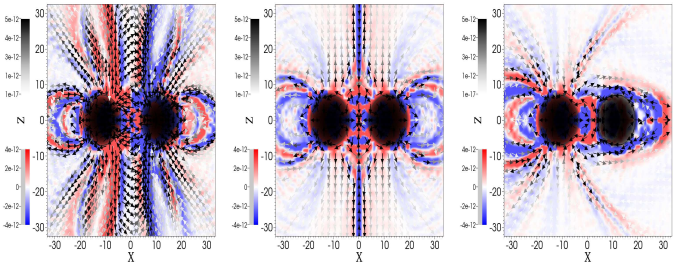

FIG. 4: Currents (drawn as arrows) and charge density (color coded) for the U/D (first panel), U/U (second panel) and U/u (third panel) cases at $t = 5.9$ ms.

Discussion: Our results reveal the late orbiting stages of binary neutron stars can induce strong electromagnetic emissions, in addition to strong gravitational wave output. These electromagnetic emissions are sourced by the ability of the magnetosphere to tap orbital energy from the system and induce both a flux of (Poynting) electromagnetic energy as well as current sheets and heat dissipation. Indeed, there may be other possible emissions coming from the current sheets produced in the U/U and U/D cases, where strong cooling can give rise to gamma-rays [24, 25] via synchrotron [25] or inverse Compton scattering [26]. (See also discussion in [27]). Interestingly, the induced current sheets are heterogeneous and have the orbital behavior strongly imprinted on them, which, in turn, could give time-varying signals that might aid in detecting these systems electromagnetically. Furthermore, accelerating fields can arise naturally at gaps [28–31], energizing a population of particles that emit high energy curvature and synchrotron radiation. Just as in the case of pulsar emissions, several of the above mentioned mechanisms might be at play to yield particular signals. Understanding which mechanism are the most important is an active area of research. At the simplest level however, if the medium is optically thick (as has been argued would be natural for the magnetic field strengths considered e.g. [10, 24]), the radiation will produce a relativistic outflow that will emit as a black body with an effective temperature given by the injection energy, in particular of Poynting luminosity. Further, recall that magnetic fields will not affect the binary dynamics provided the strengths considered are $< 10^{17}$ G. Thus, our Poynting luminosities can be rescaled in strength by $(B/10^{11}{\rm G})^2$. From our simulations we can directly extract the total Poynting luminosity emitted in a radius $r_o \approx 30$ km (at, e.g. $t \approx 5$ ms) and express the resulting temperature $T = S_{A/B}\ 10^7 B_{11}^{1/2}$ K, with the constant $S_{A/B}$ providing the value for the different cases ($S_{U/U} = 4.7$, $S_{U/u} = 2$ and $S_{U/D} = 10$). Notice that the luminosity in Case U/u, obtained from our simulations, agrees with the order of magnitude with the simple estimates by using the unipolar inductor model for the strongly magnetized star with a weakly magnetized companion in a free space magnetosphere. This leads to similar effective temperatures, when the same assumptions (optically thick magnetosphere) are considered, in the hard X-ray of the spectrum. Notice that in the extreme case where the primary star (for the U/u case) is a magnetar of $B \sim 10^{15}$ G the luminosity will increase to $L_{\rm U/u} \approx 1.6 \times 10^{47}$ erg/s, while that the black body temperature will rise up to $T_{\rm U/u} = 2 \times 10^9$ K, well inside the γ-ray range.

We have shown global magnetic fields within a binary system can give rise to a rich phenomenology that powers strong emissions on the electromagnetic side ($\simeq 10^{40-43}(B/10^{11}{\rm G})^2$ erg/s) prior to the merger, setting ideal conditions for several emission processes. These luminosities are at the level of the brightest pulsars and beyond and would bear particular characteristics tied to the orbital behavior. This, together with the power emitted in gravitational waves indicate the system is strongly radiative in multiple bands and channels. We have also identified possible features that can lead to observable signals tied to the orbital behavior of the system. The consequential time-dependent nature of possible emissions might help in their detection, especially if some prior localization (in time and space) are provided by gravitational wave information.

Acknowledgments: It is a pleasure to thank A. Broderick, J. McKinney, A. Spitkovksy for discussions and Chris Thompson for discussions and comments on the manuscript. This work was supported by the NSF under grants PHY-0969827 (LIU), PHY-0969811 (BYU) and NSERC through Discovery Grants (to LL). CP acknowledges support by the Jeffrey L. Bishop Fellowship. Research at Perimeter Institute is supported through Industry Canada and by the Province of Ontario through the Ministry of Research & Innovation. Computations were performed at XSEDE and Scinet.

[1] E. Nakar, Physics Reports **442**, 166 (2007), arXiv:astro-ph/0701748.
[2] E. Troja, S. Rosswog, and N. Gehrels, Astrophys.J. **723**, 1711 (2010), 1009.1385.
[3] L. Z. Kelley, I. Mandel, and E. Ramirez-Ruiz (2012), 1209.3027.
[4] M. Branchesi, A. Klotz, and M. Laas-Bourez (LIGO Scientific Collaboration, Virgo Collaboration) (2011), 1110.3169.
[5] B. Sathyaprakash and B. F. Schutz, Living Reviews in Relativity **12** (2009), URL `http://www.livingreviews.org/lrr-2009-2`.
[6] J. S. Bloom, D. E. Holz, S. A. Hughes, K. Menou, A. Adams, et al. (2009), 0902.1527.
[7] D. Tsang, J. S. Read, T. Hinderer, A. L. Piro, and R. Bondarescu, Physical Review Letters **108**, 011102 (2012), 1110.0467.
[8] V. M. Lipunov and I. E. Panchenko, Astron. Astrophys. **312**, 937 (1996), arXiv:astro-ph/9608155.
[9] M. Vietri, The Astrophysical Journal Letters **471**, L95 (1996).
[10] B. M. S. Hansen and M. Lyutikov, MNRAS **322**, 695 (2001), arXiv:astro-ph/0003218.
[11] A. L. Piro, Astrophys.J. **755**, 80 (2012), 1205.6482.
[12] D. Lai (2012), 1206.3723.
[13] L. Lehner, C. Palenzuela, S. L. Liebling, C. Thompson, and C. Hanna, Phys.Rev. **D86**, 104035 (2012), 1112.2622.
[14] M. Anderson, E. W. Hirschmann, L. Lehner, S. L. Liebling, P. M. Motl, D. Neilsen, C. Palenzuela, and J. E. Tohline, Physical Review Letters **100**, 191101 (2008), 0801.4387.
[15] C. Palenzuela, L. Lehner, O. Reula, and L. Rezzolla, Mon.Not.Roy.Astron.Soc. **394**, 1727 (2009), 0810.1838.
[16] C. Palenzuela, M. Anderson, L. Lehner, S. L. Liebling, and D. Neilsen, Phys. Rev. Lett. **103**, 081101 (2009), 0905.1121.
[17] S. Chawla, M. Anderson, M. Besselman, L. Lehner, S. L. Liebling, P. M. Motl, and D. Neilsen, Phys. Rev. Lett. **105**, 111101 (2010).
[18] C. Palenzuela, L. Lehner, and S. L. Liebling, Science **329**, 927 (2010), 1005.1067.
[19] D. Neilsen, L. Lehner, C. Palenzuela, E. W. Hirschmann, S. L. Liebling, et al., Proc.Nat.Acad.Sci. **108**, 12641 (2011), 1012.5661.
[20] K. Dionysopoulou, D. Alic, C. Palenzuela, L. Rezzolla, and B. Giacomazzo, ArXiv e-prints (2012), 1208.3487.
[21] LORENE. home page (2010), `http://www.lorene.obspm.fr/`.
[22] K. Ioka and K. Taniguchi, Astrophys.J. **537**, 327 (2000), astro-ph/0001218.
[23] A. Spitkovsky, Astrophys.J. Letters **648**, L51 (2006), astro-ph/0603147.
[24] D. A. Uzdensky, Space Science Reviews **160**, 45 (2011), 1101.2472.
[25] D. A. Uzdensky and A. Spitkovsky (2012), 1210.3346.
[26] M. Lyutikov, ArXiv e-prints (2012), 1208.5329.
[27] J. Arons, A&AS **120**, C49 (1996).
[28] R. W. Romani and I.-A. Yadigaroglu, Astrophys. J. **438**, 314 (1995), arXiv:astro-ph/9401045.
[29] K. S. Cheng, M. Ruderman, and L. Zhang, Astrophys. J. **537**, 964 (2000).
[30] A. G. Muslimov and A. K. Harding, Astrophys.J. **588**, 430 (2003), astro-ph/0301023.
[31] A. G. Muslimov and A. K. Harding, Astrophys.J. **606**, 1143 (2004), astro-ph/0402462.